Author's copy. Appeared in the 64th IEEE Conference on Decision and Control 2024

Guaranteeing System-level Properties in Genetic Circuits Subject to Context Effects

Inigo Incer, Ayush Pandey, Nicholas Nolan, Emma L. Peterman,
Kate E. Galloway, Eduardo D. Sontag, and Domitilla Del Vecchio

***Abstract*— The identification of constraints on system parameters that will ensure that a system achieves desired requirements remains a challenge in synthetic biology, where components unintentionally affect one another by perturbing the cellular environment in which they operate. This paper shows how to solve this problem optimally for a class of input/output system-level specifications, and for unintended interactions due to resource sharing. Specifically, we show how to solve the problem based on the input/output properties of the subsystems and on the unintended interaction map. Our approach is based on the elimination of quantifiers in monotone properties of the system. We illustrate applications of this methodology to guaranteeing system-level performance of multiplexed and sequential biosensing and of bistable genetic circuits.**

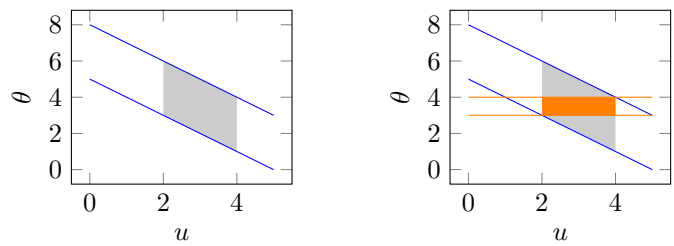

Fig. 1: To make a system satisfy (a) a specification ϕ (gray), we seek (b) restrictions on the parameter space that make the system satisfy our objectives (orange) for all inputs in a range.

I. Introduction

Synthetic biology is an engineering field that uses core biomolecular processes to develop biological circuits that achieve a desired end goal. Applications that the field impacts include medical diagnostics [1], [2], [3], regenerative medicine [4], [5], therapeutics [6], and space travel [7]. One example of a fundamental system that might be employed in these applications is the toggle switch, which can be used to implement genetic memory [8]. Designing systems like the toggle switch remains a lengthy, expensive, and time-consuming process, mostly due to the fact that genetic circuits depend on their cellular context, and that this context is in turn affected by the genetic circuits themselves [5]. A well-characterized instance of this problem is the issue of resource sharing. In particular, it has been shown that competition for resources within the cell can lead to coupling between otherwise-independent circuits, which can entirely disrupt the intended circuit's performance [9]. There has been a plethora of work in recent years to tackle this problem. Approaches fall into three main classes: insulation of circuit from context [10], [11], [12], [13], [14], making the relevant cellular context adapt to the circuit's demand [15], [16], or making the circuit adapt to a global cellular variable of interest [17]. In this paper, we consider a complementary approach to those listed above, which is to co-design multiple genetic modules (subsystems) by optimizing the subsystem's parameters. Specifically, we tackle this optimization problem such that pre-fixed system-level specifications are met.

Contributions. In this paper, we express the problem of finding constraints on the parameter space of a circuit to achieve desired system steady-state input-to-output properties in terms of quantifier elimination (QE). We provide the explicit computation of this QE problem when the system-level specifications are monotone.

Paper outline. Section II introduces a formulation of the problem of optimally constraining the parameter space of a system so that it satisfies a desired input-to-output specification, solves the problem for a class of monotone specifications, and discusses a methodology for solving the problem compositionally. In Section III, we consider applications of this methodology to guaranteeing system-level performance of multiplexed and sequential biosensing and of bistable genetic circuits. Section IV concludes the paper and outlines next steps.

II. Optimal constraints on system parameters

A critical problem in the engineering of genetic circuits is how to pick system parameters so that specifications are met. We address this problem here, even in the midst of resource competition, which causes circuit components to degrade the performance of others. In this situation, we would like to obtain the most relaxed constraints on system parameters that will yield a system that meets our goals. How should we define *most relaxed* in this context?

Example 1. To gain insight on this issue, consider a circuit with one input u and one output y. Suppose we want the circuit to have the following specification: as long as the

This work was supported by AFOSR MURI Grant #FA9550-22-1-0316 and by the ASEE and NSF through the eFellows Program.

I. Incer is with the University of Michigan, Ann Arbor, MI 48109, USA.
A. Pandey is with the University of California, Merced, CA 95343 USA.
N. Nolan, E. L. Peterman, K. E. Galloway, and D. Del Vecchio are with the Massachusetts Institute of Technology, Cambridge, MA 02139 USA.
E. D. Sontag is with Northeastern University, Boston, MA 02115 USA.

input satisfies $2 \leq u \leq 4$, the output should satisfy $5 \leq y \leq 8$. Moreover, suppose we know that $y = u + \theta$, where θ is a circuit parameter. This system specification is shown in Figure 1a. We wish to find the most relaxed requirement on θ such that if a given θ^* satisfies this requirement, then for all values of u satisfying $2 \leq u \leq 4$, the system will meet its objective. Figure 1b shows that the most relaxed specification we can place on θ is $3 \leq \theta \leq 4$. Indeed, for values of θ outside this range, there are values of u within the set $[2, 4]$ that result in the system failing to meet the top-level objective.

Generalizing this example, suppose that our system has to satisfy a specification $\phi(u, \theta)$ as long as u satisfies a condition $\sigma(u)$. The notation $\phi(u, \theta)$ means that for specific values of u and θ, we can evaluate whether the requirement $\phi(u, \theta)$ has been satisfied. Then we want to find the most relaxed constraint on θ, namely $\psi(\theta)$, such that for all θ, $\psi(\theta)$ holds if and only if for all $u \models \sigma$[1], the top-level requirement ϕ is satisfied. In other words, we seek ψ satisfying

$$\psi(\theta) \Leftrightarrow \forall u. \left(\sigma(u) \Rightarrow \phi(u, \theta)\right).$$

As shown in [18], Prop. II.1, the expression ψ given is the most relaxed specification that solves the formula $\sigma \wedge x \models \phi$. It is the *most relaxed* (or *optimal*) in the sense that, if another formula $\psi'(\theta)$ is a solution to this problem, then we must necessarily have $\psi' \models \psi$. This means that the optimal specification we can impose on θ to ensure that our system satisfies its objectives is

$$\psi(\theta) \colon \forall u. \left(\sigma(u) \Rightarrow \phi(u, \theta)\right). \tag{1}$$

The solution to (1) is provided in [18] as a general optimization problem. Next, we will obtain a closed-form expression for the solution to this problem exploiting a specific structure of the system-level requirements.

A. Constraining system-level parameters optimally

As a general framework, we will consider a circuit with m inputs u_i and n outputs y_j. Suppose we want our system to satisfy the specification $\phi(y) \colon \bigwedge_j \phi_j(y_j)$ as long as the inputs u satisfy $\sigma(u) \colon \bigwedge_i \sigma_i(u_i)$, where $\sigma_i \colon u_i \in U_i$ for given sets U_i.

Assumption 1. We will further assume that we can write $\phi_j(y_j)$ in the form $F_j(G_1^j(u_1), \ldots, G_m^j(u_m), \theta) \geq 0$, where θ is a vector with o entries and the functions $F_j(x_1, \ldots, x_m, \theta)$ are monotone in their first m arguments.

As before, we seek the most relaxed constraint ψ on the system parameters θ_i such that ϕ is satisfied when σ holds. We define

$$g_i^j = \begin{cases} \min\limits_{u \models \sigma} G_i^j(u_i) & \text{if } \frac{\partial F_j}{\partial x_i}(G_1^j(u_1), \ldots, G_m^j(u_m), \theta) \geq 0 \\ & \text{for all } u_k \models \sigma_k \\ \max\limits_{u \models \sigma} G_i^j(u_i) & \text{otherwise.} \end{cases} \tag{2}$$

[1]This notation, standard in logic, is read u *satisfies* property σ. In set notation, it is equivalent to the statement $u \in \{v \in \mathcal{U} \mid \sigma(v)\}$, where $\mathcal{U}$ is the domain of u. Also, the symbol $\wedge$ stands for conjunction.

Next, we state a lemma and our main result:

Lemma 1. *Under the assumptions just stated,* $\forall u_1.\sigma_1(u_1) \Rightarrow (F_j(G_1^j(u_1), \ldots, G_m^j(u_m), \theta) \geq 0)$ *is equivalent to* $F_j(g_1^j, G_2^j(u_2), \ldots, G_m^j(u_m), \theta) \geq 0$*, where* g_1^j *is given by* (2).

Proof. From Proposition II.3 of [18], we know that $(F_j(G_1^j(u_1), \ldots, G^j(u_m), \theta) \geq 0) \wedge \sigma_1(u_1) \models (F_j(g_1^j, G_2^j(u_2), \ldots, G_m^j(u_m), \theta) \geq 0)$ and that $(F_j(g_1, G_2^j(u_2), \ldots, G_m^j(u_m), \theta) \geq 0) \models (F_j(G_1^j(u_1), G_2^j(u_2), \ldots, G_m^j(u_m), \theta) \geq 0)$. Existentially quantifying the first formula over u_1 yields $(F_j(G_1^j(u_1), \ldots, G^j(u_m), \theta) \geq 0) \models (F_j(g_1^j, G_2^j(u_2), \ldots, G^j(u_m), \theta) \geq 0)$. The lemma follows. □

Theorem 1. *Under Assumption 1, the most relaxed specification* $\psi(\theta)$ *that ensures that the system satisfies* $\phi(y)$ *when the inputs satisfy* $\sigma(u)$ *is*

$$\psi(\theta) \colon \bigwedge_j F_j(g_1^j, \ldots, g_m^j, \theta) \geq 0,$$

where the g_i^j *are given by* (2).

Proof. We compute ψ from (1):

$$\begin{aligned} \psi \colon & \forall u. (\bigwedge_i \sigma_i(u_i) \Rightarrow \bigwedge_j \phi_j) \\ : & \bigwedge_j \forall u_1 \ldots u_m. (\bigwedge_i \sigma_i(u_i) \Rightarrow \phi_j) \end{aligned}$$

Applying Proposition II.2 of [18], yields

$$\psi \colon \bigwedge_j \forall u_2 \ldots u_m. \bigwedge_{i>1} \sigma_i(u_i) \Rightarrow (\forall u_1.\sigma_1(u_1) \Rightarrow \phi_j)$$

By Lemma 1, we get

$$\psi \colon \bigwedge_j \forall u_2 \ldots u_m. \bigwedge_{i>1} \sigma_i(u_i) \Rightarrow \begin{pmatrix} F_j(g_1^j, G_2^j(u_2), \ldots, \\ G_m^j(u_m), \theta) \geq 0 \end{pmatrix}$$

Repeatedly applying Proposition II.2 of [18] and Lemma 1 to the rest of the u variables yields the theorem. □

Remark 1. Oftentimes, our constraint σ will be of the form $\bigwedge_i u_i^L \leq u_i \leq u_i^H$. If all G_i^j are monotonically increasing, we can directly compute (2):

$$g_i^j = \begin{cases} G_i^j(u_i^L) & \frac{\partial F_j}{\partial x_i}(G_1^j(u_1), \ldots, G_m^j(u_m), \theta) \geq 0, \\ & u_k \models \sigma_k \\ G_i^j(u_i^H) & \text{otherwise.} \end{cases}$$

Theorem 1 yields the most relaxed constraints on the parameter space that solve our problem. This theorem and Remark 1 allow us to solve (1) by a simple substitution of values in ϕ for the variable we are eliminating. For instance, in Example 1, we wanted the system to meet the top-level requirement $\phi(u, \theta) \colon \phi_1 \wedge \phi_2$ when $\sigma(u, \theta) \colon 2 \leq u \leq 4$, where $\phi_1(u, \theta) \colon (u + \theta - 5 \geq 0)$ and $\phi_2(u, \theta) \colon (-u - \theta + 8 \geq 0)$. Therefore, we can solve the QE problem for ϕ by solving QE problems for ϕ_1 and ϕ_2 independently as follows: since

ϕ_1 is increasing in u, and ϕ_2 is decreasing, Remark 1 tells us that the solution to the QE problem is obtained by replacing u with its appropriate bound in each formula. We obtain the solution $\psi\colon \phi_1(2,\theta) \wedge \phi_2(4,\theta)$, which is equivalent to $(\theta \geq 3) \wedge (4 \geq \theta)$, as we obtained before.

One challenge we may face when using Theorem 1 and Remark 1 is that they require us to have a functional relationship between the top-level inputs and outputs in our system, and this relationship may not be monotone, even when the system is obtained by interconnecting components with monotone input-to-output relations. One way to preserve the monotonicity of the system-level constraints is by adding requirements on the internal signals in our systems. That is, we can add requirements to all outputs y_i of components that feed inputs u_k of other components. While adding requirements on internal signals enables us to solve for parameters using Theorem 1 and Remark 1, the resulting analysis may yield conservative results, as illustrated in the following example.

Example 2. Consider the system shown in Figure 2. Suppose we wish the top-level system to satisfy the specification $2 \leq y$ when $3 \leq u \leq 6$, knowing that $y = x + u$ and $x = -\frac{\theta}{u}$, where $\theta \in \mathbb{R}_{\geq 0}$ is a system parameter. Our objective is to compute constraints on θ that guarantee this behavior. From (1), we are interested in computing

$$\psi(\theta)\colon \forall u.\, (u \in [3,6] \Rightarrow u - \theta/u \geq 2)\,.$$

The system-level, input-to-output relation is $y = u - \theta/u$, which is not monotone in u, and therefore we cannot apply Theorem 1. For positive values of θ, we can only have $y \geq 2$ when $u \geq 1+\sqrt{1+\theta}$. To make sure that we get $y \geq 2$ when $u \geq 3$, we set $1 + \sqrt{1+\theta} \leq 3$, which yields the constraint $\theta \leq 3$. Our analysis guarantees that if θ obeys this constraint, we will obtain the desired system-level specification.

To enable the application of Theorem 1, we add a constraint on x such that our system-level specification becomes $2 \leq y$ and $x \geq -1/2$ when $3 \leq u \leq 6$. Since $x \geq -1/2$ and $u \geq 3$, we have $y = x+u \geq 3-1/2 \geq 2$, satisfying the requirement on y. To satisfy the requirement on x, we solve

$$\forall u.\, (u \in [3,6] \Rightarrow -\theta/u \geq -1/2)\,.$$

We can use Theorem 1 and Remark 1 to solve this problem, since the system level constraint can be written as $F(u) \geq 0$, where $F(u) = -\theta/u+1/2$ is monotonically increasing in u. The application of the remark yields the constraint $-\theta/3 + 1/2 \geq 0$, which is equivalent to $\theta \leq 3/2$. We observe that by adding a constraint on the intermediate signal x, our resulting constraints on θ are conservative.

III. Applications

Now we will apply the methodology outlined in Section II to compute constraints on the parameters that yield desired system-level performance in several scenarios. All results can be reproduced by executing the code that accompanies this paper[2].

[2]https://github.com/pacti-org/BioPacti/blob/main/SummarizedCaseStudies/

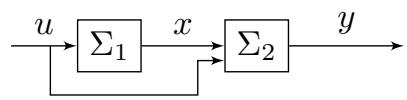

Fig. 2: A system with two components is required to satisfy a top-level specification. The input-to-output relations for both components are monotone, but the system's input-to-output relation is not.

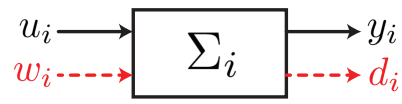

Fig. 3: Block diagram representation of a genetic module. Subsystem Σ_i takes as input u_i and w_i, and outputs y_i and d_i. Here, u_i is the intended input of the module, while input w_i is a disturbance input that captures the perturbation on the cellular resources available to this module. Similarly, y_i is the intended output, while d_i is a disturbance output that captures the load on cellular resources that system Σ_i applies [19].

A. Multiplexed biosensing in bacteria

First, we will consider the design of genetic circuits in bacteria. These circuits are formed by interconnecting subsystems. We will consider subsystem Σ_i as a genetic module encapsulating the mRNA and protein dynamics of gene expression, given inputs u_i and w_i, and outputs y_i and d_i (Figure 3). Specifically, we have mRNA m_i and protein p_i as state variables, governed by the following dynamics [19]:

$$\begin{aligned} \dot{m}_i &= T_i v_i(u_i) - \delta m_i \\ \dot{p}_i &= R_i \frac{m_i/\kappa_i}{1 + m_i/\kappa_i + w_i} - \gamma p_i, \end{aligned} \tag{3}$$

with outputs

$$y_i = p_i, d_i = m_i/\kappa_i,$$

and interconnection rule

$$w_i = \Sigma_{j \neq i} d_j. \tag{4}$$

In this model, output d_i captures the disturbance that module Σ_i applies to the cellular ribosome pool, while w_i is the cumulative perturbation to the ribosome pool that all other modules apply, thereby affecting system Σ_i. In this system, T_i is the basal transcription rate of mRNA, R_i is a lumped parameter that is proportional to both the translation rate constant, as well as the total translation resources (chiefly ribosomes) in the system, and κ_i is the tunable mRNA-ribosome binding dissociation constant. For our purposes in this paper, we consider $\theta_i := 1/\kappa_i$ as the tunable parameters used for design, which practically represent the ribosome binding site strength. This strength, in practice, is tunable by the genetic sequence of the ribosome binding site (RBS) using tools such as the RBS calculator [20]. Beyond this, δ is the degradation rate constant of mRNA, γ is the decay rate constant for proteins, and $v_i(u_i)$

is a Hill-like function describing the effect that the input u_i has on the production of mRNA. If u_i activates gene expression, $v_i(u_i)$ is a monotonically increasing function of u_i; otherwise, $v_i(u_i)$ is a monotonically decreasing function. Here, we assume that u_i activates transcription and so each v_i is a monotonically increasing function of u_i. This model of ribosome competition in the cell has been experimentally validated in [9]. We will be interested in studying the input/output steady-state characteristics of these systems.

In this section, we consider two genetic modules Σ_1 and Σ_2 working in parallel, as shown in Figure 4a. This setup is representative of a multiplexed biosensor, in which each input u_i is a biomolecule of interest, to which the system responds by generating an output signal y_i, typically a fluorescent protein [21], [22], [23], [24]. Without resource competition, the red arrows are absent in the block diagram of Figure 4a, and each output responds to its corresponding input independent of the other inputs. Multiplexed biosensors are of interest for detecting multiple different pathogens concurrently, such as for diagnostic applications, while maintaining the ability to uniquely identify each [3]. However, due to ribosome competition, when the output of one sensor increases due to its own input rising, the ouput of the second sensor declines [25]. In this section, we therefore characterize the parameter space that allows, despite ribosome competition, both sensors to keep their steady state outputs sufficiently high when their inputs are presented.

From (3) and (4) with $i \in \{1, 2\}$, we can write the steady state value of the output as:

$$y_i = \frac{c_i d_i}{1 + d_1 + d_2}, \tag{5}$$

where $c_i = R_i/\gamma$ and $d_i = \theta_i m_i = \theta_i \frac{T_i}{\delta} v_i(u_i)$. We will require our circuit to satisfy the following specification: $y_i \geq y_i^H$ when $u_i \in [u_i^H, u_i^S]$ for $i \in \{1, 2\}$. In other words, we want the outputs to exceed the thresholds y_i^H when the inputs u_i are appropriately bounded. Using (5), we express the top-level specification in terms of the u_i and θ_i:

$$\phi(u, \theta)\colon \bigwedge_i \frac{c_i \theta_i \frac{T_i}{\delta} v_i(u_i)}{1 + \theta_1 \frac{T_1}{\delta} v_1(u_1) + \theta_2 \frac{T_2}{\delta} v_2(u_2)} \geq y_i^H.$$

For the inputs, we have the specification

$$\sigma(u)\colon \bigwedge_i u_i^H \leq u_i \leq u_i^S.$$

The specification of the parameters can be obtained by applying (1). We obtain

$$\psi(\theta)\colon \forall u_1, u_2.\ (\sigma(u_1, u_2, \theta) \Rightarrow \phi(u_1, u_2, \theta)). \tag{6}$$

We observe that we can express $\phi(u, \theta)$ in the form required by Assumption 1 by setting $F_j(x_1, x_2, \theta) = \frac{c_j \theta_j x_j}{1 + \theta_1 x_1 + \theta_2 x_2} - y_i^H$ and $G_i^j(x_i) = \frac{T_i}{\delta} v_i(u_i)$. The functions F_j are monotone in both arguments x_i when the θ_i are nonnegative, which we shall assume; moreover, the G_i^j are monotonically increasing. This implies that we can solve the QE problem (6) by using Remark 1.

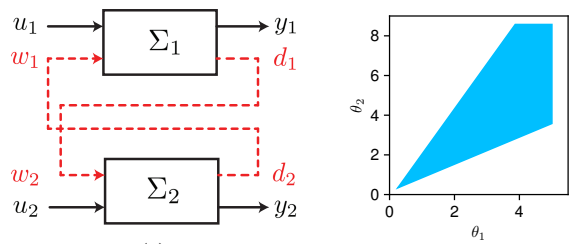

Fig. 4: Analysis of multiplexed biosensing in bacteria. (a) The system model contains two components in parallel, sharing resources. We analyze the system to obtain (b) restrictions on the set of parameters that make the system work as intended. The system-level requirements and constants that yield these results are $u_1^M = u_2^M = 0$, $u_1^L = u_2^L = 0.05$, $u_1^H = u_2^H = 4$, $u_1^S = u_2^S = 4.1$, $y_1^L = 0.2$, $y_1^H = 0.3$, $y_2^L = 0.3$, and $y_2^H = 0.4$. $c_1 = c_2 = 1$ and $T_1/\delta v_1$ and $T_2/\delta v_2$ are the identity function.

This computation yields constraints on the θ_i that ensure that the system exceeds its high thresholds y_i^H when the inputs lie in the range $[u_i^H, u_i^S]$. We can carry out a similar, independent analysis to compute constraints on the parameters θ_i that will ensure that the system does not exceed low thresholds y_i^L when the inputs lie in the range $[0, u_i^L]$. Figure 4b shows the computation of constraints on the parameters θ_i to yield both high and low thresholds for the outputs y for a given set of requirements and constants.

B. Sequential signal processing in bacteria

Now we consider a series of two systems, as shown in Figure 5a. This signal cascade is a common motif in many biological circuits, as it can be used to either amplify a signal or introduce delay into a signal [26]. In this topology, however, even if each genetic module Σ_i has a monotonically increasing input/output behavior, the composition of the two systems may not share this property, on account of ribosome competition [9]. Here, we wish to design our system parameters to ensure that, for high inputs, the system output is above a threshold and for low inputs, the system output is below a threshold.

The mathematical model of this system is as in (3) and (4), with $i \in \{1, 2\}$. We wish to consider the steady state of our system, for which we find:

$$y_i = \frac{c_i d_i}{1 + d_1 + d_2}. \tag{7}$$

where $c_i = R_i/\gamma$ and $d_i = \theta_i m_i = \theta_i \frac{T_i}{\delta} v_i(u_i)$ for the parameters defined in (3). Also, we have $u_1 := u$ and $u_2 := y_1$, as the systems are connected in series. It is shown in [27] that systems of this form have a unique, stable equilibrium point. The question is to find restrictions on the space of parameters θ_i that will yield $y_2 \geq y_2^H$ in the steady state when u satisfies $u^S \geq u \geq u^H$.

As discussed in Section II, to keep the system constrains monotone, we will introduce a system-level requirement for the signal y_1, namely, we will also require that $y_1^H \leq y_1 \leq y_1^S$. When introducing this requirement, y_1 becomes both an output and input variable of the system for the following reason: by assuming bounds on y_1, we obtain bounds on d_2, which contributes to bound y_1 again. This behavior in our analysis stems from the fact that there is a feedback loop in our system. Thus, we express our top-level requirement ϕ in terms of *inputs* u and y_1 and the parameters θ_i using (7). We obtain the system specification $\phi(u, y_1, \theta_1, \theta_2)\colon \wedge_{i=1}^{3} \phi_i(u, y_1, \theta_1, \theta_2)$ given by

$$\phi_1\colon \left(\frac{y_1^H}{c_1} \leq \frac{\theta_1 \frac{T_1}{\delta} v_1(u)}{1 + \theta_1 \frac{T_1}{\delta} v_1(u) + \theta_2 \frac{T_2}{\delta} v_2(y_1)} \right)$$

$$\phi_2\colon \left(\frac{\theta_1 \frac{T_1}{\delta} v_1(u)}{1 + \theta_1 \frac{T_1}{\delta} v_1(u) + \theta_2 \frac{T_2}{\delta} v_2(y_1)} \leq \frac{y_1^S}{c_1} \right)$$

$$\phi_3\colon \left(\frac{y_2^H}{c_2} \leq \frac{\theta_2 \frac{T_2}{\delta} v_2(y_1)}{1 + \theta_1 \frac{T_1}{\delta} v_1(u) + \theta_2 \frac{T_2}{\delta} v_2(y_1)} \right).$$

We have the following bounds on the input variables:

$$\sigma(u, y_1)\colon \left(u^S \leq u \leq u^S\right) \wedge \left(y_1^H \leq y_1 \leq y_1^S\right).$$

Our objective is to obtain the most relaxed constraints on the parameters θ_i such that ϕ holds when σ holds. This most relaxed specification is given by applying (1):

$$\psi(\theta_1, \theta_2)\colon \forall u, y_1.\ (\sigma(u, y_1) \Rightarrow \phi(u, y_1, \theta_1, \theta_2)). \quad (8)$$

We observe that we can apply Theorem 1 and Remark 1 to solve this problem for the following reason: We can express ϕ_1 as $\phi_1\colon F_1(G_1^j(u), G_2^1(y_1)) \geq 0$ with $F_1(x_1, x_2, \theta_1, \theta_2) = \frac{\theta_1 x_1}{1+\theta_1 x_1+\theta_2 x_2} - \frac{y_1^H}{c_1}$ and $G_i^1(\cdot) = T_i/\delta v_i(\cdot)$. F_1 is monotone in both arguments when the θ_i are nonnegative, which we shall assume; we also have that the G_i^1 are monotonically increasing. A similar reasoning applies to ϕ_2 and ϕ_3. This implies that Assumption 1 holds, and we can solve (8) by variable substitution using Remark 1. After solving for the constraints on the θ_i that guarantee that we will have $y_2 \geq y_2^H$ when $u^H \leq u \leq u^S$, we consider further constraints on the θ_i that also guarantee that the system output y_2 will remain below a threshold y_2^L when the top level input u is below a threshold u^L. We use a similar procedure to compute these constraints. Figure 5b shows the result of computing the parameter specifications that guarantee both thresholds simultaneously for fixed values of requirements and system constants. Figures 5c and 5d show the input-to-output behavior of system when implemented by using parameters θ_i that satisfy the constraints of Figure 5b. We observe that the system-level performance satisfies the objective specifications. Details of the implementation can be found in the accompanying code[2].

C. Bistable genetic circuit

Next, we consider the design of a bistable circuit to demonstrate that the framework to compute a parameter space that satisfies specifications is sufficiently general to capture more sophisticated specifications, such as bistability.

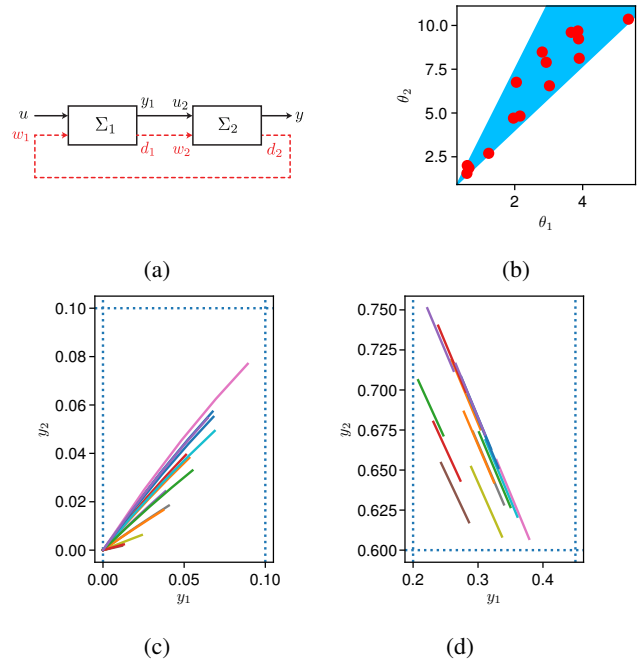

Fig. 5: Analysis of sequential signal processing in bacteria. (a) The system model contains two elements in series, sharing resources. With our analysis, we obtain (b) restrictions on the set of parameters for desired system behavior. The red dots indicate samples extracted from the parameter space to verify the satisfaction of the system requirements. We simulate the circuit as u varies from (c) 0 to u_L and from (d) u^H to u^S. Each plot in (c) and (d) corresponds to one parameter sampled from the region (b). The system-level requirements and constants that yield these results are $c_1 = c_2 = 1$, $u^M = 0$, $u^L = 1$, $u^H = 10$, $u^S = 100$, $y_1^m = 0$, $y_1^L = 0.1$, $y_1^H = 0.2$, $y_1^S = 0.45$, $y_2^L = 0.1$, $y_2^H = 0.6$, $T_1 v_1(u^M)/\delta = 0$, $T_1 v_1(u^L)/\delta = 0.02$, $T_1 v_1(u^H)/\delta = 4$, $T_1 v_1(u^S)/\delta = 5$, $T_2 v_2(y_1^M)/\delta = 0$, $T_2 v_2(y_1^L)/\delta = 0.01$, $T_2 v_2(y_1^H)/\delta = 4.1$, and $T_2 v_2(y_1^S)/\delta = 4.15$.

For simplicity, we do not consider resource sharing in this example, but the analysis can be readily extended to such a case. Multistable circuits are important for development and differentiation in mammalian cells. We consider a bistable circuit design reported by Lebar *et al* [28], which utilizes both mutual inhibition and positive feedback between two genes to generate two stable states as shown in Figure 6. Such models with bistable attractor states have been used to explain transcription factor-induced differentiation in mammalian cell fate decisions [29].

The variables, m_i and m_j, represent the mRNA molecules produced from transcription of subsystems Σ_i and Σ_j, respectively. Each of these mRNA molecules encodes an activator (A_i, A_j) that implements positive transcriptional feedback and a repressor (R_i, R_j) that inhibits transcription of the opposite gene. For this system, we modify the definition of each subsystem Σ_i from the previous sections, so that we have the following dynamics:

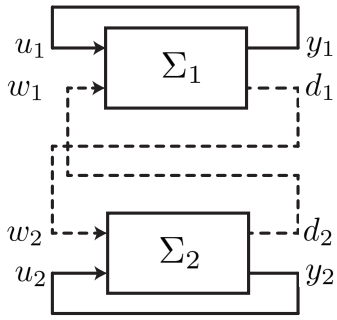

Fig. 6: Schematic of a genetic circuit with two genes in mammalian cells comprising self activation and mutual inhibition. Solid lines represent activation, and dashed lines are repression.

Model parameter values

Parameter	Value
a_i	0.5
k_i	1
a'_i	10
k'_i	1
a_j	1
d_j	1
a'_j	10
d'_j	1
κ	20
δ	1
γ	0.05

Threshold constants

Parameter	Value
$y^H_{i_2}$	45
$y^L_{j_2}$	0.02
$y^H_{i_1}$	1
$y^L_{j_1}$	5×10^{-4}
$y^H_{j_2}$	90
$y^L_{i_2}$	0.05
$y^H_{j_1}$	0.25
$y^L_{i_1}$	1×10^{-3}

TABLE I: Numerical values for parameters and constants.

$$\begin{aligned} \dot{m}_i &= \left(\alpha_{0,i} + \alpha_i \frac{a_i u_i}{k_i}\right) \frac{D_{i_{\text{tot}}}}{1 + \frac{a_i u_i}{k_i} + \frac{a'_i w_i}{k'_i}} - \delta m_i \\ \dot{A}_i &= \kappa m_i - \gamma A_i \\ \dot{R}_i &= \kappa m_j - \gamma R_i, \end{aligned} \tag{9}$$

with outputs:

$$y_i = (m_i, A_i), d_i = R_i,$$

and input/interconnection rule:

$$u_i = y_{i_2}, w_i = \Sigma_{j \neq i} d_j.$$

In this model, $\alpha_{0,i}$ and α_i represent leaky and transcription factor-induced transcription, respectively, for module Σ_i. For the promoter of genetic module Σ_i, the binding kinetics of activator u_i are given by a_i and k_i, and the binding kinetics of the repressor w_i are given by a'_i and d'_i. $D_{i_{\text{tot}}}$ represents the copy number of the gene in module Σ_i. Finally, κ represents the mRNA translation rate constant, δ is the mRNA degradation rate constant, and γ is the protein degradation rate constant.

Under certain parameter regimes, this circuit has two stable steady states with high levels of either y_{i_2} or y_{j_2} as well as one unstable steady state with intermediate levels of both activator proteins. Here, we compute parameter ranges under which the two stable steady states are within a certain domain. Since the repressors d_j are expressed from the same mRNA molecule as the activator y_{i_2}, we assume that they have the same dynamics. Thus, we analyze a 4-state model with $y_{i_1}, y_{j_1}, y_{i_2}$, and y_{j_2} variables, which is obtained by setting $y_{i_2} = d_j$ in the dynamics of system (9).

1) Specifications: We want to analyze the region of the parameter space where the system shows two stable steady states. Our design parameters are $\alpha_{0,i}$, the basal transcription rate, α_i, the activated transcription rate, and $D_{i,tot}$, the total gene copy number. These parameters were chosen as they are easily experimentally tuned through promoter design and genetic cargo delivery. We assume that the other parameters in the model (a_i, a'_i, k_i, k'_i, δ, and γ) are fixed to a constant value. Further, we note that to achieve bistable behavior we must have $a_i/k_i \neq a'_i/k'_i$. For this problem, we state the system specification by first describing the top-level input-output system specifications.

Our general strategy is to first determine parameter conditions that guarantee the co-existence of two steady states in correspondence of high y_{i_1}, y_{i_2} with low y_{j_1}, y_{j_2} and low y_{i_1}, y_{i_2} with high y_{j_1}, y_{j_2}. To provide an analysis approach that is generally applicable in any dimension, we do not rely on algebraically computing the system's steady state. Rather, we rely only on the monotonicity properties of the system dynamics. As such, we write the system specifications that impose two conditions for the concurrent presence of two equilibria:

$$\begin{aligned} &\left(y_{i_1} \geq y^H_{i_1} \wedge y_{j_1} \leq y^L_{j_1} \wedge y_{i_2} \geq y^H_{i_2} \wedge y_{j_2} \leq y^L_{j_2}\right) \vee \\ &\left(y_{i_1} \leq y^L_{i_1} \wedge y_{j_1} \geq y^H_{j_1} \wedge y_{i_2} \leq y^L_{i_2} \wedge y_{j_2} \geq y^H_{j_2}\right) \end{aligned} \tag{10}$$

where $y^H_{i_1}, y^H_{i_2}, y^L_{j_1}, y^L_{j_2}$ are thresholds for the first equilibrium point where y_{i_1} and y_{i_2} are in the "on" state and y_{j_1} and y_{j_2} are in the "off" state of the circuit. Similarly, we have thresholds for the other equilibrium, $y^L_{i_1}, y^L_{i_2}, y^H_{j_1}, y^H_{j_2}$ that specifies the second requirement. We use nominal parameter values for all parameters other than the design parameters shown in Table I.

With these parameter values, we observe that system nullclines exhibit bistable behavior with three equilibrium points out of which two are stable and one is unstable. Using the nullcline analysis, we also choose values for the threshold parameters introduced above $y^H_{i_2}, y^L_{j_2}, y^H_{i_1}, y^L_{i_1}, y^H_{j_2}, y^L_{i_2}, y^H_{j_1}$, and $y^L_{i_1}$ (see Table I). We visualize the threshold parameters overlaid on the nullclines and the region for the top-level system specification in Figure 7.

2) Exploiting monotonic dynamics to derive feasible parameters: Our goal is to find feasible regions for the design parameters such that the necessary requirements described by ϕ for bistable equilibria are satisfied. We write the steady state conditions of the system as:

$$\begin{aligned} \left(\alpha_{0,i} + \alpha_i \frac{a_i y_{i_2}}{k_i}\right) \frac{D_{i_\text{tot}}}{1 + \frac{a_i y_{i_2}}{k_i} + \frac{a'_i y_{j_2}}{k'_i}} &= \delta y_{i_1} \\ \kappa y_{i_1} &= \gamma y_{i_2}. \end{aligned} \tag{11}$$

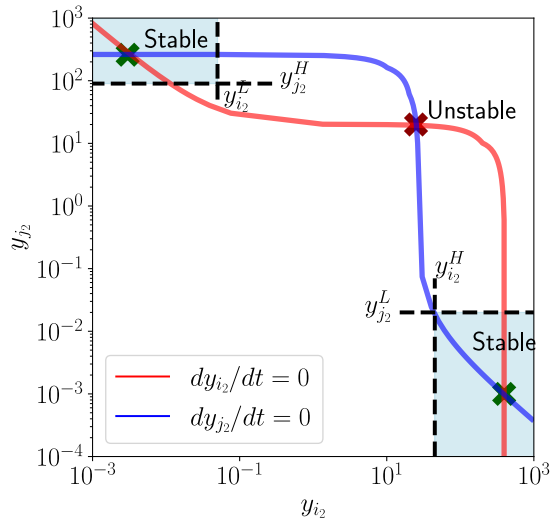

Fig. 7: The nullclines for nominal system dynamics and an overlay of the threshold constants used to define the system specifications. The nullclines are plotted in log-log scale.

We introduce new parameters $p_i := \alpha_{0,i} D_{i_\text{tot}}$ and $q_i := \alpha_i D_{i_\text{tot}}$ which lump our design parameters. We also define new constants $b_i = a_i/k_i$ and $b'_i = a'_i/k'_i$ for brevity. Then, in addition to (11), the steady-state conditions become:

$$\frac{p_i + b_i q_i y_{i_2}}{1 + b_i y_{i_2} + b'_i y_{j_2}} = \delta y_{i_1}, \tag{12}$$

where $i \neq j$. Now we start analyzing the constraints on the parameters p_i and q_i that will make the system achieve $y_{i_1} \geq y_{i_1}^H \wedge y_{j_1} \leq y_{j_1}^L \wedge y_{i_2} \geq y_{i_2}^H \wedge y_{j_2} \leq y_{j_2}^L$.

We can express these requirements using (11) and (12) in order to start setting up the problem in such a way that we can apply Theorem 1 to obtain constraints for the system parameters. One difficulty with this approach, however, is that (12) is not necessarily monotone in y_{i_2}. As a result, we add two additional top-level constraints that ensure that this function is monotone by requiring that the derivative of (12) with respect to y_{i_2} be positive. Thus, the top-level requirement $\phi(y, p, q)$ is given by

$$\phi\colon \left(\frac{p_i + b_i q_i y_{i_2}}{1 + b_i y_{i_2} + b'_i y_{j_2}} \geq \delta y_{i_1}^H\right) \wedge \tag{13}$$

$$\left(\frac{p_j + b_j q_j y_{j_2}}{1 + b_j y_{j_2} + b'_j y_{i_2}} \leq \delta y_{j_1}^L\right) \wedge \tag{14}$$

$$\left(\kappa y_{i_1} \geq \gamma y_{i_2}^H\right) \wedge \left(\kappa y_{j_1} \leq \gamma y_{j_2}^L\right) \wedge \tag{15}$$

$$\left(q_i(1 + b'_i y_{j_2}) \geq p_i\right) \wedge \left(q_j(1 + b'_j y_{i_2}) \geq p_j\right), \tag{16}$$

where (13) and (14) come from (12); (15) comes from (11); and (16) comes from requiring (12) to be monotonically increasing in y_{I_2} for $I \in \{i, j\}$.

We also have the constraints

$$\sigma(y_{i_1}, y_{i_2}, y_{j_1}, y_{j_2})\colon \left(y_{i_1} \geq y_{i_1}^H\right) \wedge \left(0 \leq y_{j_1} \leq y_{j_1}^L\right) \wedge \left(y_{i_2} \geq y_{i_2}^H\right) \wedge \left(0 \leq y_{j_2} \leq y_{j_2}^L\right).$$

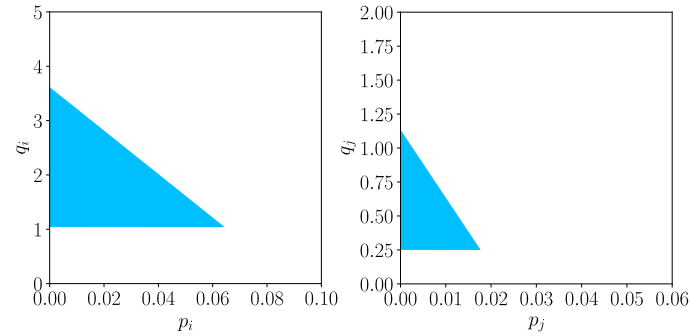

Fig. 8: The feasibility regions for the design parameters: p_i, p_j, q_i, q_j.

We compute the constraints on the p_i and q_i that yield the desired system-level behaviors by using (1). We want to compute

$$\psi(p, q)\colon \forall y_{i_1}, y_{i_2}, y_{j_1}, y_{j_2}.\, (\sigma(y) \Rightarrow \phi(y, p, q)). \tag{17}$$

To compute this QE, we verify whether Assumption 1 holds. We already observed that (13) and (14) can be understood as monotonic in both arguments y_{i_2} and y_{j_2} because of the addition of requirement (16). The two expressions in (15) are clearly monotonic functions. Since all predicates are monotone, we can apply Theorem 1 and Remark 1 to solve (17). We obtain the region

$$\begin{aligned} 0.042p_i + 0.94q_i &\geq 1, \\ 0.002p_j + 4.4e-05q_j &\leq 5 \times 10^{-5}, \\ p_i - q_i &\leq 0, \\ p_j - 451q_j &\leq 0. \end{aligned}$$

Repeating the process above for the condition in the second line of (10), where $y_{i_1} \leq y_{i_1}^L, y_{j_1} \geq y_{j_1}^H$ and $y_{i_2} \leq y_{i_2}^L, y_{j_2} \geq y_{j_2}^H$ gives similar inequalities that bound the region of feasible values. Merging these conditions by taking the intersection, we obtain the final bounds on the design parameters. For the chosen parameter values, we visualize these feasibility bounds in 2D graphs in Figure 8.

Finally, to verify our predictions on feasible bounds on the design parameters, we choose a range of values of parameters from the feasibility regions and plot the nullclines to assess bistability. All sampled values of parameters from the feasibility regions lead to bistable behavior as visualized with nullclines in Figure 9.

IV. Conclusions and Future Work

This paper considered the computation of constraints on system parameters with the objective of ensuring that the system satisfies an input-to-output requirement. We expressed the computation of the optimal solution for this problem in terms of quantifier elimination. We provided a method to solve this problem by replacing variables when the system-level objective is given in terms of monotone functions. Applications to guaranteeing system-level performance of multiplexed and sequential biosensing and of bistable genetic

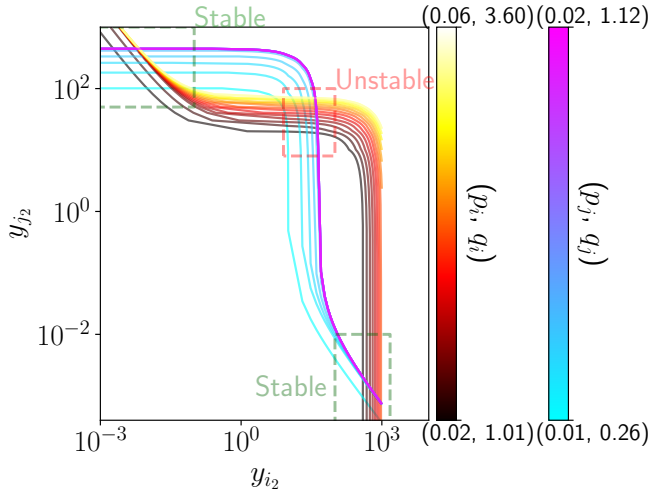

Fig. 9: Prediction of system behavior using parameter values sampled from the computed feasibility regions. The intersecting nullclines show equilibrium points, and for all feasible values we observe three such intersections out of which two are stable equilibria (the regions are denoted). The numerical values of the parameters of interest (p_i, p_j) and (q_i, q_i) are shown on color maps. All other parameters are set at nominal values given in Table I. The plot is shown in log-log scale.

circuits showed the viability of the approach. Future work includes the analysis of more complex biological circuits (such as multi-stable systems) and experimental validations.

Acknowledgements

We are grateful to Richard M. Murray for helpful conversations over the course of this project. I. Incer was with the California Institute of Technology during the completion of this work.

References

[1] K. Pardee, A. A. Green, M. K. Takahashi, D. Braff, G. Lambert, J. W. Lee, T. Ferrante, D. Ma, N. Donghia, M. Fan *et al.*, "Rapid, low-cost detection of zika virus using programmable biomolecular components," *Cell*, vol. 165, no. 5, pp. 1255–1266, 2016.

[2] K. Pardee, A. A. Green, T. Ferrante, D. E. Cameron, A. DaleyKeyser, P. Yin, and J. J. Collins, "based synthetic gene networks," *Cell*, vol. 159, no. 4, pp. 940–954, 2014.

[3] D. T. Riglar, T. W. Giessen, M. Baym, S. J. Kerns, M. J. Niederhuber, R. T. Bronson, J. W. Kotula, G. K. Gerber, J. C. Way, and P. A. Silver, "Engineered bacteria can function in the mammalian gut long-term as live diagnostics of inflammation," *Nature biotechnology*, vol. 35, no. 7, pp. 653–658, 2017.

[4] K. Ilia, N. Shakiba, T. Bingham, R. D. Jones, M. M. Kaminski, E. Aravera, S. Bruno, S. Palacios, R. Weiss, J. J. Collins *et al.*, "Synthetic genetic circuits to uncover the oct4 trajectories of successful reprogramming of human fibroblasts," *Science Advances*, vol. 9, no. 48, p. eadg8495, 2023.

[5] M. Tewary, N. Shakiba, and P. W. Zandstra, "Stem cell bioengineering: building from stem cell biology," *Nature Reviews Genetics*, vol. 19, no. 10, pp. 595–614, 2018.

[6] S. Chowdhury, S. Castro, C. Coker, T. E. Hinchliffe, N. Arpaia, and T. Danino, "Programmable bacteria induce durable tumor regression and systemic antitumor immunity," *Nature medicine*, vol. 25, no. 7, pp. 1057–1063, 2019.

[7] A. J. Berliner, I. Lipsky, D. Ho, J. M. Hilzinger, G. Vengerova, G. Makrygiorgos, M. J. McNulty, K. Yates, N. J. Averesch, C. S. Cockell *et al.*, "Space bioprocess engineering on the horizon," *Communications Engineering*, vol. 1, no. 1, p. 13, 2022.

[8] T. S. Gardner, C. R. Cantor, and J. J. Collins, "Construction of a genetic toggle switch in escherichia coli," *Nature*, vol. 403, no. 6767, pp. 339–342, 2000.

[9] Y. Qian, H.-H. Huang, J. I. Jiménez, and D. Del Vecchio, "Resource competition shapes the response of genetic circuits," *ACS synthetic biology*, vol. 6, no. 7, pp. 1263–1272, 2017.

[10] H.-H. Huang, Y. Qian, and D. Del Vecchio, "A quasi-integral controller for adaptation of genetic modules to variable ribosome demand," *Nature communications*, vol. 9, no. 1, p. 5415, 2018.

[11] R. D. Jones, Y. Qian, V. Siciliano, B. DiAndreth, J. Huh, R. Weiss, and D. Del Vecchio, "An endoribonuclease-based feedforward controller for decoupling resource-limited genetic modules in mammalian cells," *Nature communications*, vol. 11, no. 1, p. 5690, 2020.

[12] R. D. Jones, Y. Qian, K. Ilia, B. Wang, M. T. Laub, D. Del Vecchio, and R. Weiss, "Robust and tunable signal processing in mammalian cells via engineered covalent modification cycles," *Nature communications*, vol. 13, no. 1, p. 1720, 2022.

[13] T. Frei, F. Cella, F. Tedeschi, J. Gutiérrez, G.-B. Stan, M. Khammash, and V. Siciliano, "Characterization and mitigation of gene expression burden in mammalian cells," *Nature communications*, vol. 11, no. 1, p. 4641, 2020.

[14] J. Gutiérrez Mena, S. Kumar, and M. Khammash, "Dynamic cybergenetic control of bacterial co-culture composition via optogenetic feedback," *Nature Communications*, vol. 13, no. 1, p. 4808, 2022.

[15] A. P. Darlington, J. Kim, J. I. Jiménez, and D. G. Bates, "Dynamic allocation of orthogonal ribosomes facilitates uncoupling of co-expressed genes," *Nature communications*, vol. 9, no. 1, p. 695, 2018.

[16] C. Barajas, H.-H. Huang, J. Gibson, L. Sandoval, and D. Del Vecchio, "Feedforward growth rate control mitigates gene activation burden," *Nature Communications*, vol. 13, no. 1, p. 7054, 2022.

[17] F. Ceroni, R. Algar, G.-B. Stan, and T. Ellis, "Quantifying cellular capacity identifies gene expression designs with reduced burden," *Nature methods*, vol. 12, no. 5, pp. 415–418, 2015.

[18] I. Incer, A. Benveniste, R. M. Murray, A. Sangiovanni-Vincentelli, and S. A. Seshia, "Context-aided variable elimination for requirement engineering," *arXiv preprint arXiv:2305.17596*, 2023.

[19] Y. Qian and D. Del Vecchio, "Mitigation of ribosome competition through distributed srna feedback," in *2016 IEEE 55th Conference on Decision and Control (CDC)*. IEEE, 2016, pp. 758–763.

[20] H. M. Salis, E. A. Mirsky, and C. A. Voigt, "Automated design of synthetic ribosome binding sites to control protein expression," *Nature biotechnology*, vol. 27, no. 10, pp. 946–950, 2009.

[21] A. J. Meyer, T. H. Segall-Shapiro, E. Glassey, J. Zhang, and C. A. Voigt, "Escherichia coli "marionette" strains with 12 highly optimized small-molecule sensors," *Nature chemical biology*, vol. 15, no. 2, pp. 196–204, 2019.

[22] C. Grazon, R. C. Baer, U. Kuzmanović, T. Nguyen, M. Chen, M. Zamani, M. Chern, P. Aquino, X. Zhang, S. Lecommandoux *et al.*, "A progesterone biosensor derived from microbial screening," *Nature communications*, vol. 11, no. 1, p. 1276, 2020.

[23] A. G. Rottinghaus, C. Xi, M. B. Amrofell, H. Yi, and T. S. Moon, "Engineering ligand-specific biosensors for aromatic amino acids and neurochemicals," *Cell systems*, vol. 13, no. 3, pp. 204–214, 2022.

[24] Y.-K. Lin and Y.-C. Yeh, "Dual-signal microbial biosensor for the detection of dopamine without inference from other catecholamine neurotransmitters," *Analytical chemistry*, vol. 89, no. 21, pp. 11 178–11 182, 2017.

[25] A. Gyorgy, J. I. Jiménez, J. Yazbek, H.-H. Huang, H. Chung, R. Weiss, and D. Del Vecchio, "Isocost lines describe the cellular economy of genetic circuits," *Biophysical journal*, vol. 109, no. 3, pp. 639–646, 2015.

[26] D. Del Vecchio and R. M. Murray, *Biomolecular feedback systems*. Princeton University Press Princeton, NJ, 2015.

[27] C. McBride and D. Del Vecchio, "The number of equilibrium points of perturbed nonlinear positive dynamical systems (extended version)," Tech. Rep., 2019.

[28] T. Lebar, U. Bexeljak *et al.*, "A bistable genetic switch based on designable dna-binding domains," *Nature Communications*, 2014.

[29] S. Huang, Y.-P. Guo, G. May, and T. Enver, "Bifurcation dynamics in lineage-commitment in bipotent progenitor cells," *Developmental biology*, vol. 305, no. 2, pp. 695–713, 2007.